

The Three-mm Ultimate Mopra Milky Way Survey. III. A Catalog of the Southern Molecular Cloud Physical Properties

Audra K. Hernandez¹, Peter J. Barnes², Ana Duarte-Cabral³, Erik Muller⁴, & Bob Benjamin⁵

1. University of Wisconsin – Madison, 2. University of Florida, 3. Cardiff University, 4. National Astronomical Observatory of Japan, 5. University of Wisconsin-Whitewater

Email: hernande@astro.wisc.edu

Summary

The Three-mm Ultimate Mopra Milky Way Survey (ThrUMMS) provides a uniform and unbiased mapping of a $60^\circ \times 2^\circ$ region of our Galaxy's southern plane (fourth-quadrant) in three CO isotopologues and CN. We present a new catalog of southern molecular clouds identified from the ^{13}CO ($J=1-0$) data. We have applied the SCIMES (Spectral Clustering for Interstellar Molecular Emission Segmentation; Colombo et al. 2015) dendrogram algorithm to the ^{13}CO ($1-0$) emission line data to construct our molecular cloud catalog, while exploring two different types of cloud extraction criteria. First, we compiled an Intensity based cloud extraction (I_{ex}) by applying SCIMES to the ^{13}CO ($1-0$) emission data, focusing on $6^\circ \times 2^\circ$ sectors at a time. The ^{13}CO ($1-0$) data has been binned to a velocity resolution of ~ 0.37 km/s, an $\sim 1'$ spatial resolution ($24'$ binning). We have used an RMS noise limit of $\sigma \sim 0.8$ K per channel to construct the dendrogram tree. Although the ThrUMMS data has a limited sensitivity due to its fast mapping techniques (see Barnes et al. 2015), we are still interested in cataloging larger cloud complexes (e.g., giant molecular cloud scale). Thus, we set a 2.5σ detection limit to maximize the connection between structures as continuous lower intensity levels and used a 4σ minimum difference between neighboring leaf peaks for them to be considered separate. The SCIMES configuration was set to consider both intensity and volume during clustering (see Colombo et al. 2015). Secondly, we were inspired by current galactic disk and molecular cloud models (cite) that generally define cloud structures based on simulated mass or mass density data cubes. To perform a column density based extraction (N_{ex}), we converted the ^{13}CO ($1-0$) intensity data into CO column density cubes by estimating the excitation temperature (T_{ex}) in each voxel from the ^{13}CO ($1-0$) data. The SCIMES detection and clustering limits from the I_{ex} extraction were also used by converted to column density limits assuming a mean cloud voxel T_{ex} of 7 K. Below we present some preliminary results of molecular clusters and their derived physical properties and dynamics:

- For the I_{ex} extraction method we find a total of 6,338 molecular clouds, of which 589 are clusters (i.e., comprised of at least 2 dendrogram leaves). For the N_{ex} extraction, we find a total of 25,891 molecular clouds, of which 3310 are clusters.
- Cluster kinematic distances were estimated using the Galactic rotation model of Reid et al. (2009). Figure 1 presents the estimated near and far kinematic distance for each I_{ex} molecular cluster as projected onto the plane of the Southern Milky Way. We find that that the overall spatial distribution of the clouds does align with the Galactic spiral structure. However, future analysis to resolve the near/far ambiguity may resolve this issue.
- We present the positions and extents of the molecular clusters identified by SCIMES in both the I_{ex} and N_{ex} extractions (Fig 2). We find that the N_{ex} extraction results in a larger number of identified clouds than the I_{ex} extraction, including a larger number of single leaf clouds. Additionally, we matched the I_{ex} and N_{ex} clusters catalogs using a coordinate-position criteria of 0.05° radius and a velocity range of ± 2.5 km/s, yielding 488 matched clouds. An initial analysis of these matched clusters shows that the N_{ex} clusters are more clumpy with ~ 5 times the number of leaves as their I_{ex} component (Fig 3a). This result was expected given that the intensity distribution is flatter than the opacity corrected column density distribution.
- A direct comparison of the matched I_{ex} and N_{ex} clusters' physical parameters suggests a one-to-one relationship. We compare effective circular radius, estimated from the SCIMES derived major and minor, finding a linear relationship with a slope of 0.994 and a Pearson coefficient of $\rho=0.994$ (Fig 3b). We then estimated the cloud masses using the $n^{12}\text{CO}/n^{13}\text{CO}$ abundance model from Milam et al. (2005) and an $n_{12}\text{CO}/n_{13}\text{CO}$ abundance of 2×10^4 (Lacy et al. 1994). Similarly, a comparison of the cloud masses yield a strong linear relationship with a slope of 0.994 and $\rho=0.999$ using the near distances, and a slope of 0.995 and $\rho=0.996$ for the far distances (Fig 3c).
- We analyzed the dynamical state of the molecular clusters. For the I_{ex} clusters, we find the power-law relation $\sigma/R^{1/2} \propto \Sigma^{\alpha_{\text{vir}}}$ (e.g. Heyer et al. 2009) with $n=2.11 \pm 0.10$ for the near distance clusters, and $n=2.92 \pm 0.21$ (Fig. 4). These indices are larger than that expected for virialized clouds ($n_{\text{vir}}=0.5$). However, we find mean virial parameters of $\log(\alpha)=0.40 \pm 0.51$ (near) and $\log(\alpha)=-0.063 \pm 0.513$. Additionally, if we force a power-law index of $n=0.5$, we estimate mean virial parameters of $\log(\alpha)=0.40$ (near) and $\log(\alpha)=-0.064$ (far), suggesting that the whole population is nearly consistent with virial equilibrium.

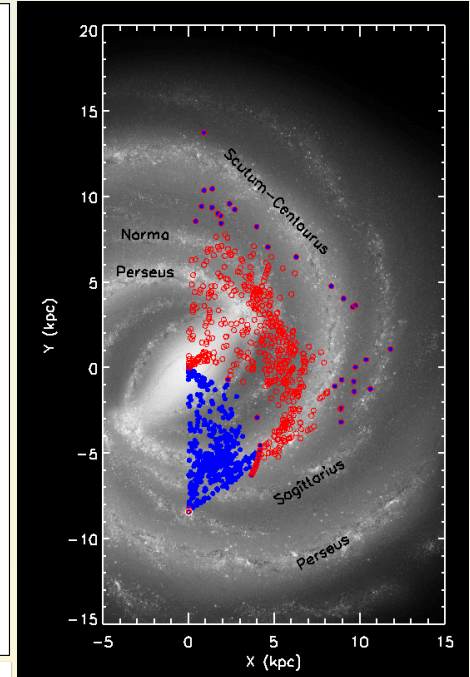


Figure 1: The spatial distribution of the I_{ex} extracted SCIMES molecular clusters overlaid on a face-on Milky Way composite image (Robert Hurt of the Spitzer Science Center with consultation from Bob Benjamin). Cluster center positions are shown for both the near (blue closed points) and far (red open points). The location of the Sun ($R_{\odot}=8.4$ kpc) is shown by the white \odot symbol.

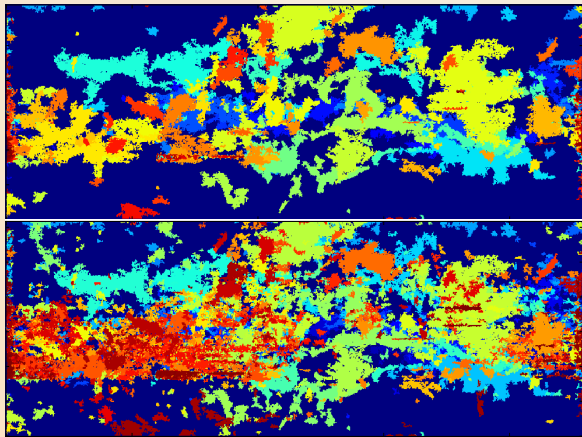


Figure 2: The positions and extents of the SCIMES molecular clouds, including single leaves, projected onto l - b space. The I_{ex} extraction clouds are shown in the top panel, while the N_{ex} extraction clouds are displayed on the bottom panel. Both bounding boxes represent one ThrUMMS $6^\circ \times 2^\circ$ sector, ranging $l=300$ - 336° and $|b|=\pm 1^\circ$. All clouds are shaded with an individual color corresponding to their SCIMES ID (left-hand scale bars).

Figure 3: Comparisons of the 488 matched I_{ex} and N_{ex} clusters. (a) Histogram of the number of N_{ex} dendrogram leaves vs. I_{ex} dendrogram leaves. The N_{ex} clusters have ~ 5 times the number of leaves as their matched I_{ex} clusters. (b) A direct comparison of the matched clusters' effective radii suggests a one-to-one relationship. (c) A comparison clusters' total mass (near: blue solid points; far: red open points) also suggest a strong linear relationship between the clusters derived from I_{ex} and N_{ex} extraction.

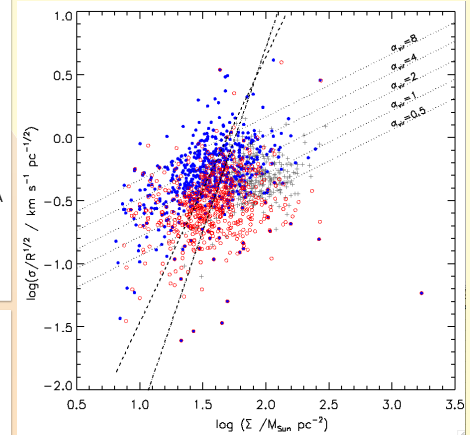
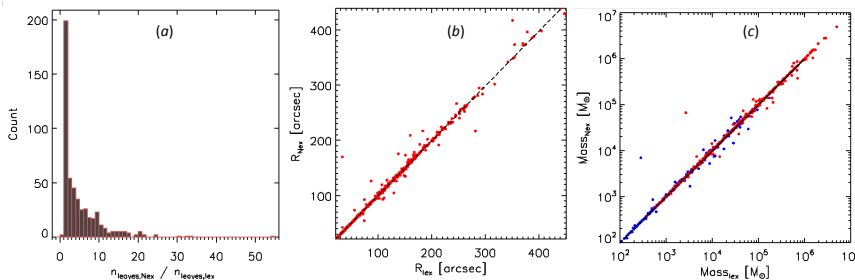


Figure 4: Dependence of $\sigma/R^{1/2}$ with mass surface density, Σ , for both the I_{ex} near (blue solid points) and far (red open points) populations. The error bar represents the estimated mean uncertainties of $\sim 14\%$ in $\sigma/R^{1/2}$ and 30% in Σ . The best-fit power-law relation for both cloud populations are shown by the black dashed lines. The dotted lines represent the different scaling relation for virialized clouds with $\alpha_{\text{vir}}=0.5, 1, 2, 4, \text{ and } 8$.

References

Acknowledgements

A.K.H acknowledges support from the National Science Foundation under grant AST-1517573. This work make use of molecular line data from the ThrUMMS Survey.

